JCB Article

APP processing is regulated by cytoplasmic phosphorylation

Ming-Sum Lee,[1] Shih-Chu Kao,[1] Cynthia A. Lemere,[2] Weiming Xia,[2] Huang-Chun Tseng,[1] Ying Zhou,[1] Rachael Neve,[3] Michael K. Ahlijanian,[4] and Li-Huei Tsai[1]

[1]Department of Pathology, Harvard Medical School and Howard Hughes Medical Institute, Boston, MA 02115
[2]Center for Neurologic Diseases, Brigham and Women's Hospital, Harvard Medical School, Boston, MA 02115
[3]Department of Psychiatry, Harvard Medical School, McLean Hospital, Belmont, MA 02478
[4]Department of CNS Discovery, Pfizer Central Research, Groton, CT 06340

Amyloid-β peptide (Aβ) aggregate in senile plaque is a key characteristic of Alzheimer's disease (AD). Here, we show that phosphorylation of amyloid precursor protein (APP) on threonine 668 (P-APP) may play a role in APP metabolism. In AD brains, P-APP accumulates in large vesicular structures in afflicted hippocampal pyramidal neurons that costain with antibodies against endosome markers and the β-secretase, BACE1. Western blot analysis reveals increased levels of T668-phosphorylated APP COOH-terminal fragments in hippocampal lysates from many AD but not control subjects. Importantly, P-APP cofractionates with endosome markers and BACE1 in an iodixanol gradient and displays extensive colocalization with BACE1 in rat primary cortical neurons. Furthermore, APP COOH-terminal fragments generated by BACE1 are preferentially phosphorylated on T668 verses those produced by α-secretase. The production of Aβ is significantly reduced when phosphorylation of T668 is either abolished by mutation or inhibited by T668 kinase inhibitors. Together, these results suggest that T668 phosphorylation may facilitate the BACE1 cleavage of APP to increase Aβ generation.

Introduction

Extracellular deposition of amyloid-β peptide (Aβ) aggregates in the brain represents a defining pathologic feature of Alzheimer's disease (AD; Price et al., 1995). Aβ is derived from proteolytic cleavage of amyloid precursor protein (APP), a type I transmembrane glycoprotein that belongs to a protein family that also includes APP-like protein (APLP) 1 and 2. Either α- or β-secretase initiates APP processing by cleaving the extracellular/lumenal domain, generating soluble NH_2-terminal fragments, sAPPα or sAPPβ, and a membrane-anchored 83-residue or 99/89-residue COOH-terminal fragments (αCTFs or βCTFs), respectively (De Strooper and Annaert, 2000). Subsequently, the membrane-bound fragments are cleaved by γ-secretase in the transmembrane region, resulting in the production of p3 (from αCTFs) or the amyloidogenic peptides Aβ40 or Aβ42 (from βCTFs).

Pharmacological and biochemical studies have shown that β- and γ-secretases are aspartyl proteases (Wolfe et al., 1999; Yan et al., 1999). β-Secretase (BACE 1) and its homologue BACE2 are type I integral membrane glycoproteins (Sinha et al., 1999; Vassar et al., 1999; Yan et al., 1999). BACE1 constitutes the primary β-secretase activity in the brain and is primarily localized within the Golgi and endosomal compartments where the acidic pH is optimal for secretase activities. To date, there is no known genetic linkage between mutations in BACE genes and AD. However, BACE1 proteins and activities have been found to be increased in AD brain regions affected by amyloid deposition, suggesting its role in AD pathogenesis (Fukumoto et al., 2002; Holsinger et al., 2002; Yang et al., 2003).

Presenilin proteins (PS1 and PS2) are integral components of the γ-secretase directly responsible for the activity of γ-secretase (Steiner and Haass, 2000). Importantly, missense mutations within PS genes are associated with familial forms

M.-S. Lee and S.-C. Kao contributed equally to this work.

The online version of this paper contains supplemental material.

Address correspondence to Li-Huei Tsai, Dept. of Pathology, Harvard Medical School and Howard Hughes Medical Institute, 200 Longwood Ave., Boston, MA 02115. Tel.: (617) 432-1053. Fax: (617) 432-3975. email: li-huei_tsai@hms.harvard.edu

Key words: Alzheimer's disease; amyloid precursor protein; BACE1; endosomes; Aβ

Abbreviations used in this paper: Aβ, amyloid-β peptide; AD, Alzheimer's disease; APLP, APP-like protein; APP, amyloid precursor protein; CTF, COOH-terminal fragment; HSV, herpes simplex virus; MS, mass spectrometry; P-APP, APP phosphorylated on threonine 668; PNS, postnuclear supernatant; PS, presenilin.

of AD. These mutations result in increased production of Aβ42, accelerating the formation of senile plaques (Hardy and Crook, 2001). PS proteins are mostly localized in the endoplasmic reticulum, Golgi apparatus (Kovacs et al., 1996; De Strooper et al., 1997), and endosomes (Lah and Levey, 2000).

Aβ has been shown to be generated in both the secretory and endocytic pathways of transfected cell lines and cultured neurons (Selkoe et al., 1996; Perez et al., 1999; Nixon et al., 2000). It is thought that Aβ can first be generated in the TGN. Remaining unprocessed APP is then transported to the cell surface where it is either cleaved by the nonamyloidogenic α-secretase or reinternalized into the endosomes, where Aβ generation has also been found. Disturbances in neuronal endocytic pathway are among the earliest known intracellular changes occurring in sporadic AD (Nixon et al., 2000). In hippocampal neurons of these AD patients, endosomes are abnormally enlarged; a change that may precede clinical symptoms, appearing before substantial Aβ accumulation. As such, abnormalities associated with the endocytic pathway have been postulated to play a significant role in amyloidogenesis (Cataldo et al., 2000).

How APP is targeted to the subcellular compartments containing its processing enzymes remains to be elucidated. Subcellular APP trafficking may be regulated by its phosphorylation. APP contains eight potential phosphorylation sites in its cytoplasmic domain. Low level phosphorylation of T654 and S655 (human APP695 isoform numbering) has been found in rat brain (Oishi et al., 1997). These two amino acids are part of the ^{653}YTSI^{656} motif, which acts as an endocytic and/or basolateral sorting signal, YXXI, in MDCK cells (Lai et al., 1998; Zheng et al., 1998). Tyrosine kinases, TrkA and c-Abl, have been shown to phosphorylate Y682 in vitro (Tarr et al., 2002). The ^{682}YENPTY^{687} motif is a canonical endocytic signal for membrane-associated receptors and mutations of Y682, N684, or P685 have been shown to inhibit the internalization of APP and decrease the generation of secreted sAPP and Aβ (Perez et al., 1999; Steinhilb et al., 2002).

Threonine 668 (T668) in the cytoplasmic domain of APP is also phosphorylated in vivo by a number of protein kinases, including GSK3β, SAPK1b/JNK3, Cdc2, and Cdk5 (Suzuki et al., 1994; Aplin et al., 1996; Iijima et al., 2000; Standen et al., 2001). Many of these kinases are associated with neurotoxicity and implicated in neurodegenerative diseases. A solution NMR study suggests that T668 phosphorylation results in significant conformational change that may affect the interactions of APP with its binding partners (Ramelot and Nicholson, 2001). As such, this phosphorylation may serve to regulate the intracellular trafficking and metabolism of APP.

Here, we provide evidence that T668 phosphorylated APP is significantly increased in AD brains. APP phosphorylated on threonine 668 (P-APP) and BACE1 colocalize in enlarged endosomes of AD hippocampal neurons and cultured primary cortical neurons. P-APP and BACE1 from mouse brain homogenates cofractionate in iodixanol gradients. Mutation of T668 to alanine (T668A) decreases this cofractionation. Furthermore, the COOH-terminal fragments of APP generated by BACE1 cleavage, βCTFs (C99/C89), are preferentially phosphorylated over the α-secretase cleavage product, αCTF (C83). Accordingly, Aβ generation is significantly reduced by mutation of T668 to alanine or by treatment using T668 kinase inhibitors. Together, these observations suggest that T668 phosphorylation may facilitate β-secretase cleavage of APP and generation of Aβ peptides.

Results

T668 phosphorylation is up-regulated in AD brains

To investigate P-APP in normal and disease brain samples, we generated a rabbit polyclonal antibody against a phospho-T668 containing peptide (αP-T668). We carefully characterized these antibodies and confirmed that the αP-T668 specifically recognized P-APP in vitro and in rat brain lysates (Fig. S1, available at http://www.jcb.org/cgi/content/full/jcb.200301115/DC1). Next, we used αP-T668 for immunohistochemistry to determine the T668 phosphorylation status of APP in AD brain samples (case information in Table S1, available at http://www.jcb.org/cgi/content/full/jcb.200301115/DC1). The overall staining patterns of P-APP in age-matched control and AD brains differed markedly (Fig. 1, A–E). Intense staining was observed in AD hippocampal pyramidal neurons (Fig. 1, B and D). Pre-adsorption of the antibody with the P-T668 containing peptide, but not the unphosphorylated peptide, completely eliminated the staining (Fig. S2, A–C, available at http://www.jcb.org/cgi/content/full/jcb.200301115/DC1). Alkaline phosphatase pretreatment of AD hippocampal sections abolished αP-T688 staining (Fig. S2, Da and b). Both mammalian APP homologues, APLP1 and APLP2 contain a homologous phosphorylated threonine in their cytoplasmic domains. Pre-adsorption of αP-T668 with phosphorylated APLP1 or APLP2 peptides containing these sites did not affect the staining pattern produced by this antibody (Fig. S2, Ea–d) making it unlikely that the αP-T668 staining in AD brains was due to phosphorylation of APLP1 or APLP2. Together, these results indicate that the αP-T668 specifically labels structures containing T668 phosphorylated APP in AD brains.

We have examined the localization of P-APP in a total of 24 AD and 11 nondemented age-matched control cases. In general, two structures that displayed strong P-T668 staining were large, vesicular bodies within the cell soma of hippocampal neurons (Fig. 1 D) and dystrophic neurites associated with amyloid plaques (Fig. 1, E–I). We also determined the distribution of P-APP in the brains of 18 mo-old APPsw Tg mice and found that αP-T668 labeled dystrophic neurites that are closely associated with amyloid plaques (Fig. S2, F–I). However, no vesicular staining in the cell body is observed. Thus, in the mouse model for amyloid plaques, P-APP is only present in one of the two compartments where it is enriched in AD.

T668 phosphorylated APP accumulates in neurons positive for phospho-Tau

Double immunostaining of P-APP and phospho-Tau (AT8) revealed a high coincidence of staining within neurons from AD (Fig. 1 J). Among 1,373 neurons surveyed that were positive for P-T668, AT8 or both, 81% were double positive, 3% were only positive for P-T668 and 16% were only positive for AT8. Of the neurons positive for AT8 only, most represented extracellular tangles that were remnants of degenerated neurons. This observation indicates that afflicted neurons in AD exhibit increased levels of P-APP. Although

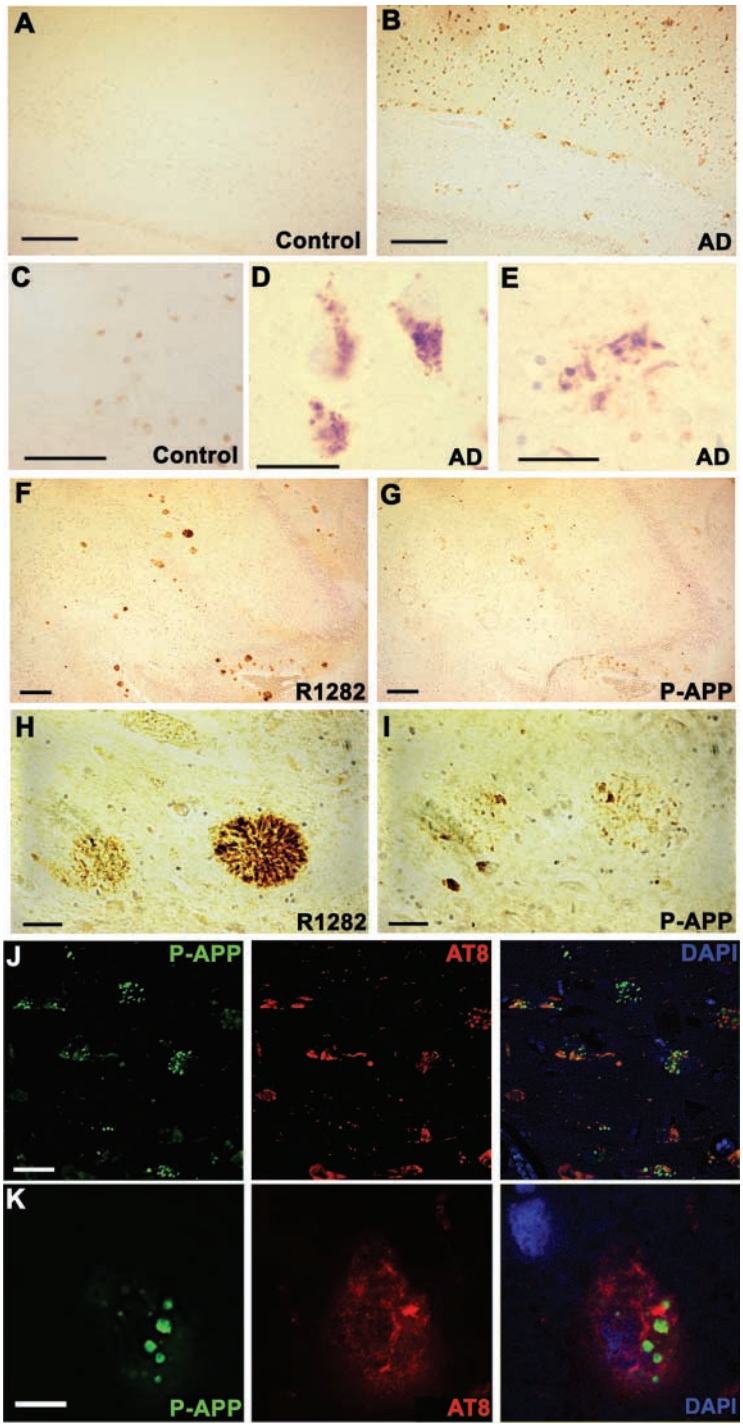

Figure 1. **T668 phosphorylated APP is elevated in human AD brains.** (A) Age-matched control hippocampal section stained with αP-T668. (B) AD hippocampal section stained with αP-T668. Strong immunoreactivity is detected in pyramidal neurons and some plaque structures in the CA fields. (C–E) Higher magnification view of hippocampal sections. (C) Age-matched control brain. (D) Pyramidal neurons containing enlarged vesicular structures positive for P-T668. (E) P-T668–positive dystrophic neurites. (F–I) αP-T668 labels dystrophic neurites that are closely associated with amyloid plaques in AD brains. (F and H) R1282 (an Aβ antibody) staining of AD hippocampal section showing the distribution of amyloid plaques. (G and I) Adjacent section stained with αP-T668 antibody showing P-T668–positive dystrophic neurites surrounding the plaques. (J and K) DeltaVision deconvolution images showing staining of P-APP and phospho-Tau (AT8) on AD brain sections. P-APP is enriched in the same neurons that have increased phospho-Tau staining. Bars: (A and B) 500 μm; (C–E) 15 μm; (F and G) 250 μm; (J) 20 μm; and (H, I, and K) 5 μm.

P-APP and phospho-Tau were present in the same neurons, they exhibited distinct subcellular localization; P-APP was present in vesicular compartments, whereas phospho-Tau was associated with filamentous structures (Fig. 1 K).

Phosphorylation of COOH-terminal fragments of APP in AD brains

To further investigate the phosphorylation of T668 in AD, we performed Western blot analysis on hippocampal tissues from 14 AD and 10 age-matched control brains (Fig. 2 A; case information in Table S2, available at http://www.jcb.org/cgi/content/full/jcb.200301115/DC1). No significant difference in levels of P-T668 on full-length APP was observed between AD and control brains. However, we found P-T668 on the APP CTFs to be considerably increased in 8 of 14 AD brains.

To determine phosphorylation sites of APP CTFs, in addition to T668, we immunoprecipitated APP from AD hippocampal lysates using αP-T668, resolved and trypsin digested the APP CTFs in a SDS-PAGE, and analyzed the tryptic fragments using MALDI-TOF mass spectrometry (MS). A summary of recovered peptides and a representative MS spectrum of tryptic digests are shown in Fig. 2 (B and C). The recovered peptides spanned the entire APP βCTF region. The presence of peptides 596–612, 596–624, 602–

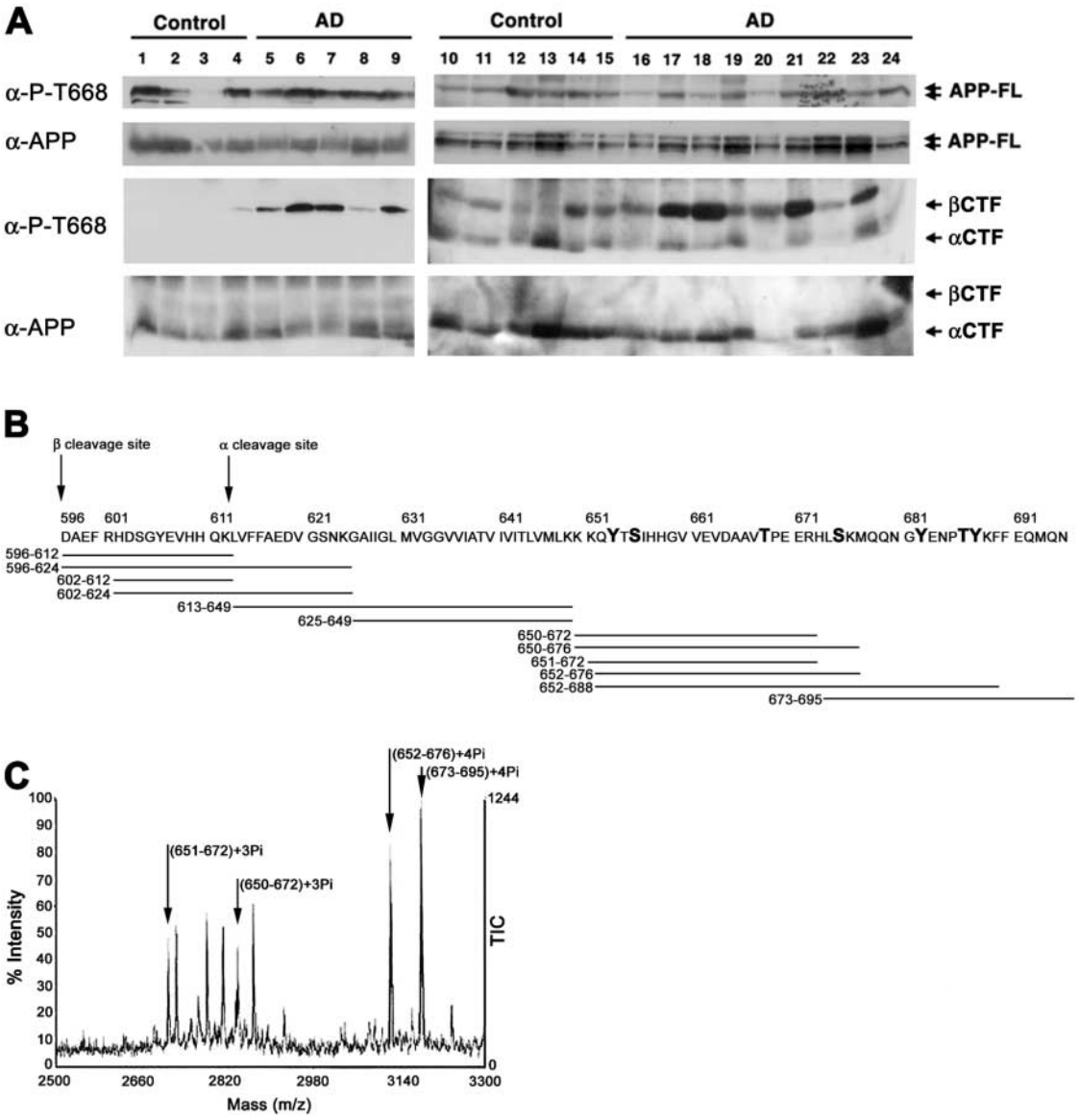

Figure 2. **The CTFs of T668 phosphorylated APP is elevated in AD brains.** (A) Western blots of brain lysates from control and AD hippocampal tissues probed with αP-T668 or an antibody against the COOH terminus of APP (C1/6.1). (B) Schematic diagram of peptides detected by mass spectrometric analysis. APP immunoprecipitated by αP-T668 from AD brain tissue was separated on SDS-PAGE, digested with trypsin, and analyzed by MALDI-TOF MS. Identified peptides are illustrated. The numbering of residues is based on APP695. The phosphorylated residues in the cytoplasmic domain of APP are in bold. (C) A partial MS spectrum showing hyperphosphorylation of the COOH terminus of APP. MS peaks representing phosphorylated tryptic peptides derived from APP are indicated (arrows).

612 and 602–624 indicated the existence of βCTF (C99). However, as trypsin also cleaves at the α-secretase site, we cannot rule out the presence of αCTF or other species of APP CTFs in the MS samples. Treatment of samples with alkaline phosphatase before MS analysis significantly reduced the intensities of the phospho-peptide signals and resulted in new ion peaks appearing at m/z positions representing dephosphorylated peptides, confirming that these peptides were indeed phosphorylated (unpublished data).

Interestingly, we found that peptides spanning residues 650–672 and 651–672 contained three phosphates per peptide. Peptides 652–676 and 673–695 contained four phosphates per peptide (Fig. 2 C). The sequence composition of the peptide ion with m/z 3123 (peptide 652–676) was selected and analyzed by postsource decay MS. We found that Y653, S655, and T668 were phosphorylated, based on the presence of corresponding y-ions and a phospho-tyrosine immonium ion (unpublished data). Furthermore, the recovery of peptide 673–695 with four phosphates suggested that all potential sites (S675, Y682, T686, and Y687) were phosphorylated (Fig. 2 C). These results indicate that in AD brains, APP CTFs contain at least seven different sites that can be phosphorylated, including T668. As a control, we isolated APP CTFs from neuroblastoma CAD cells overexpressing human APP using an APP COOH-terminal antibody. We found two phospho-peptides (peptides 651–672 and 650–672) containing three phosphates per peptide, indicating that three out of four potential sites (Y653, T654, S655,

and T668) were phosphorylated. We did not detect any signal representing peptide 673–695, which contained four potential phosphorylation sites (S675, Y682, T686, and Y687; see Fig. S3, available at http://www.jcb.org/cgi/content/full/jcb.200301115/DC1). This result showed that analogous phospho-peptides of APP CTFs detected in AD brain samples were also present in recombinant APP expressing CAD cells. Moreover, as many potential sites were not phosphorylated in APP expressing cells, it supports the notion that the cytoplasmic domain of APP is hyperphosphorylated in AD. Because the phosphorylated residues include serines, threonines and tyrosines, this observation suggests that multiple protein kinases are involved in APP phosphorylation in AD.

T668 phosphorylated APP is enriched in endocytic compartments and colocalized with BACE1 in AD brains

The large vesicular structures positive for P-APP have not been described previously (Fig. 1 D). To determine the nature of this structure, we performed double immunofluorescence staining on AD hippocampal sections with a large panel of organelle markers. As αP-T668 recognizes both full-length APP and APP CTFs, immunostaining using this antibody represents localization of both forms of APP phosphorylated on T668. We found that P-APP–positive vesicles could be labeled by the endosome markers Rab4 (Fig. 3 A), Rab5 (Fig. 3 B), and EEA1 (Fig. 3 C), but not by the lysosome markers cathepsin D (Fig. 3 D) or cathepsin B (Fig. S4 A, available at http://www.jcb.org/cgi/content/full/jcb.200301115/DC1), the synaptic vesicle marker SV2 (not depicted), the Golgi markers GM130 or MannII (not depicted), or the ER markers Bip/Grp78 (not depicted) or GP96 (Fig. S4 B). These costaining results indicate that P-APP is enriched in the endocytic compartments of AD hippocampal neurons.

We also examined the presence of APP processing enzymes in the P-APP–positive vesicles. Interestingly, the staining of β-secretase BACE1 was robust in the P-APP–positive neurons. Furthermore, BACE1 displayed extensive colocalization with P-APP (Fig. 3 E). A second BACE1 anti-

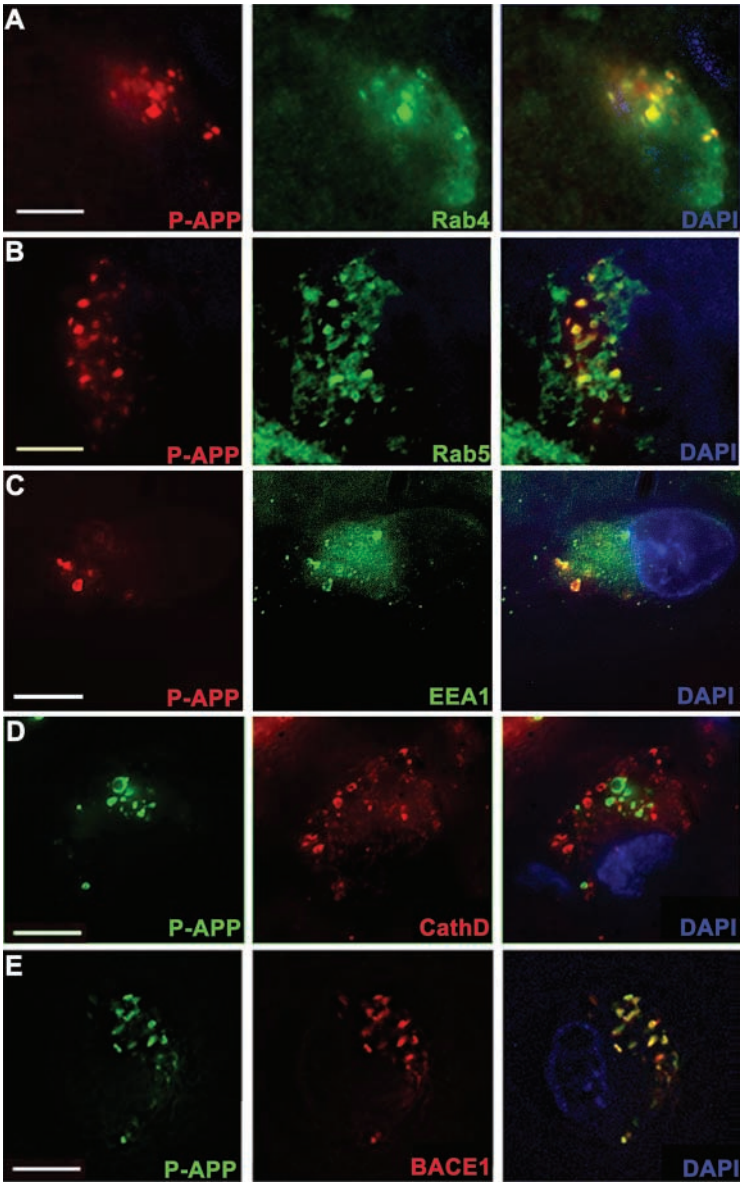

Figure 3. **Subcellular localization of P-APP in AD brain sections.** (A–D) P-APP is localized to endocytic compartments but not lysosomes in AD brains. T668 phosphorylated APP colocalizes with endocytic vesicle markers: (A) Rab4, (B) Rab5, and (C) EEA1, but not with the lysosome marker, (D) cathepsin D. (E) Colocalization of T668 phosphorylated APP and BACE1 in the enlarged vesicles in AD brains. Bars, 5 μm.

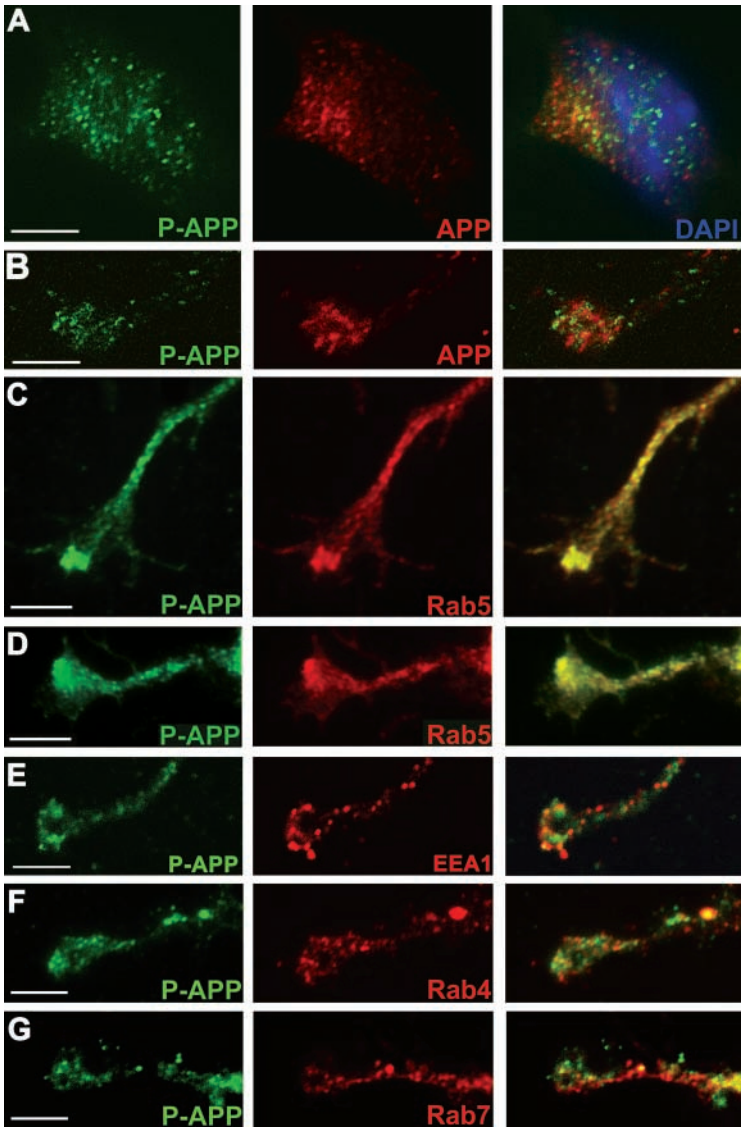

Figure 4. **Subcellular localization of P-APP in cultured primary cortical neurons.** Double immunofluorescence staining of rat primary cortical neurons. (A and B) Costaining of P-APP and regular APP (C1/6.1) in the (A) soma and (B) growth cone. (C and D) Colocalization of P-APP and Rab5 in the growth cones. (E–G) Costaining of P-APP and (E) early endosome marker EEA1, (F) recycling endosome marker Rab4, and (G) late endosome marker Rab7. Bars, 5 μm.

body gave rise to similar staining pattern in AD brain sections (unpublished data). Antibodies to PS1 did not specifically label the P-APP–positive vesicles in AD brain sections (unpublished data). These data suggest that P-APP colocalizes with BACE1 in enlarged endosomes in AD brains.

Colocalization of T668 phosphorylated APP and BACE1 in primary neurons

To further determine the subcellular distribution of P-APP and its physiological relationship with BACE1, we performed double immunostaining on normal rat primary cortical neurons. In these neurons, P-APP signal appeared punctate in the soma and growth cones with a distribution pattern somewhat distinct from that of regular APP (Fig. 4, A and B). Interestingly, P-APP showed substantial colocalization with the early endosome marker Rab5 in the growth cones (Fig. 4, C and D). Modest overlap between P-APP and EEA1 (early endosome marker; Fig. 4 E), Rab4 (recycling endosome marker; Fig. 4 F), Rab7 (late endosome marker; Fig. 4 G) or adaptin-γ (TGN marker; Fig. S5 A, available at http://www.jcb.org/cgi/content/full/jcb.200301115/DC1) was observed. There was little colocalization between GM130 (cis-Golgi marker; Fig. S5 B) and P-APP. Interestingly, P-APP and BACE1 displayed extensive colocalization in the growth cones of young neurons (Fig. 5, A and B) and showed partial colocalization in neurites of 10-d-old cultured neurons (Fig. S5, C and D). Only limited colocalization of regular APP and BACE1 was observed (Fig. 5 C). P-APP and PS1 also showed little colocalization in the growth cones (Fig. 5 D).

We further performed immunoisolation experiments to characterize P-APP, APP, and BACE1 containing vesicles (Fig. 5 E). We found that Rab5 was present in P-APP, APP, and BACE1 immunoisolates. Previous studies have shown that APP is present in the TGN (Annaert et al., 1999). However, we did not detect GM130 in any of the immunoisolates. In addition, the levels of BACE1 in P-APP immunoisolates were higher than those in APP immunoisolates, indicating that T668 phosphorylated APP preferentially colocalized with BACE1. Together, these experiments suggest that P-APP is in the same subcellular

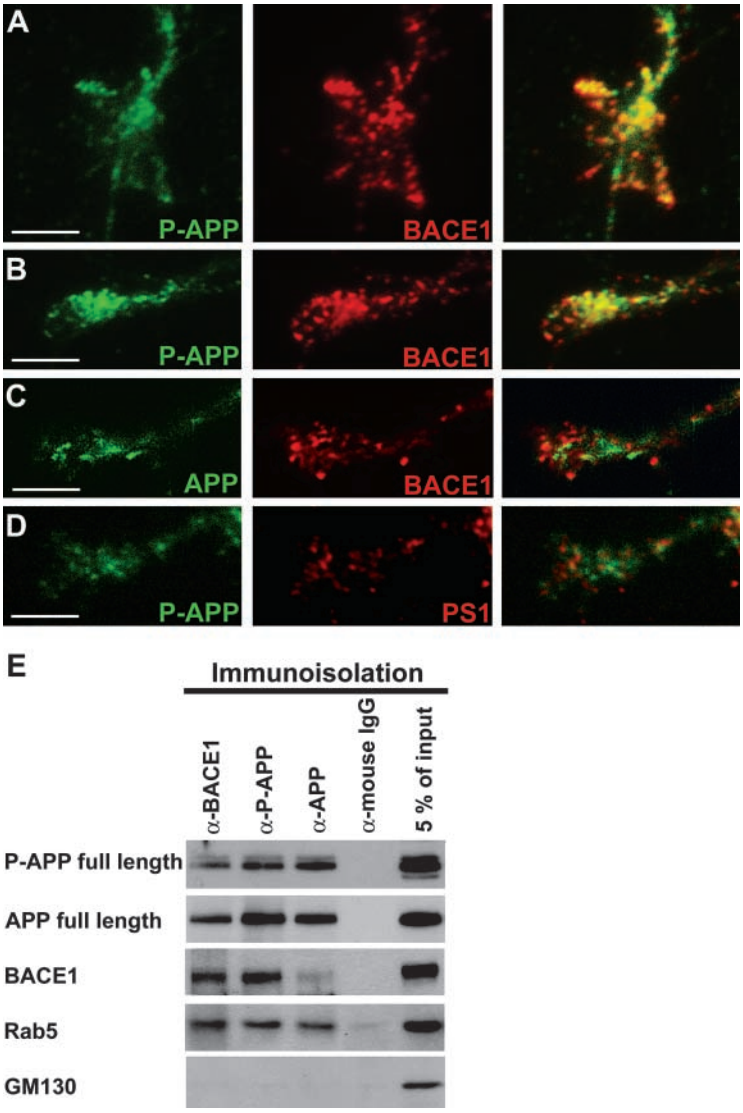

Figure 5. **T668 phosphorylated APP colocalizes with BACE1 in primary cortical neurons.** (A and B) Costaining of P-APP and BACE1 in the growth cones. (C) Costaining of regular APP (C1/6.1) and BACE1 in the growth cone. (D) Costaining of P-APP and Presenilin 1(PS1) in the growth cone. Bars, 5 μm. (E) Immunoisolation of P-APP, APP, and BACE1 containing vesicles. Vesicular organelles were immunoisolated from mouse brain homogenates using M-280 Dynabeads conjugated to anti–P-T668, anti-APP, or anti-BACE1 antibodies. Immunoisolates were examined by Western blot analysis.

compartment as the APP processing enzyme BACE1, in both AD brains and cultured neurons.

T668 phosphorylated APP cofractionates with BACE1 and endosome markers in an iodixanol step gradient

Next, we performed biochemical fractionations to gain additional insight into the subcellular localization of P-APP. Organelles in an adult wild-type mouse brain were separated through an iodixanol step gradient (Fig. 6 A). Western blot analysis using the APP COOH-terminal antibody showed that full-length APP had a broad distribution between fractions 8–20. Full-length P-APP displayed a more restricted profile between fractions 8–16. We also detected P-APP signal in the bottom of the gradient (fractions 21–23). As the gradient was bottom loaded, this likely represented unsegregated lysates, or possibly, the presence of immature, less glycosylated P-APP in the early secretory pathway. P-APP CTFs had a very discrete distribution spanning fractions 9–13, whereas APP CTFs were present between fractions 8–16. The APP CTFs detected by the αP-T668 displayed a higher molecular size than those detected by the APP COOH-terminal antibody, indicating that αP-T668 might preferentially label the β-secretase product(s) of APP.

Organelle markers revealed that Rab5 displayed a broad distribution, which overlapped with P-APP. Lysosomes, as identified by cathepsin D, also displayed a broad distribution, which was shifted to the right of the gradient. The Golgi apparatus (GM130) and ER (Bip) segregated to the bottom of the gradient. Digitalization and plotting of the Western blot signals of fractions 1–20 revealed that full-length APP, P-APP and BACE1 largely cosegregated in fractions 8–13 of iodixanol gradient with the APP signal extended to the heavier fractions of the gradient (Fig. 6 B).

To assess the significance of T668 phosphorylation in APP subcellular localization, we introduced wild-type and T668A mutant APP into primary cortical neurons using recombinant herpes simplex virus (HSV). 20 h after infection, cell homogenates were fractionated through iodixanol step gradient and the distribution of APP was analyzed. Interestingly, wild-type APP exhibited more extensive cosegregation with BACE1 than the T668A mutant APP, which was shifted to the heavier fractions of the gradient (Fig. 6 C; immunoblots in Fig. S6 A, available at http://www.jcb.org/cgi/content/

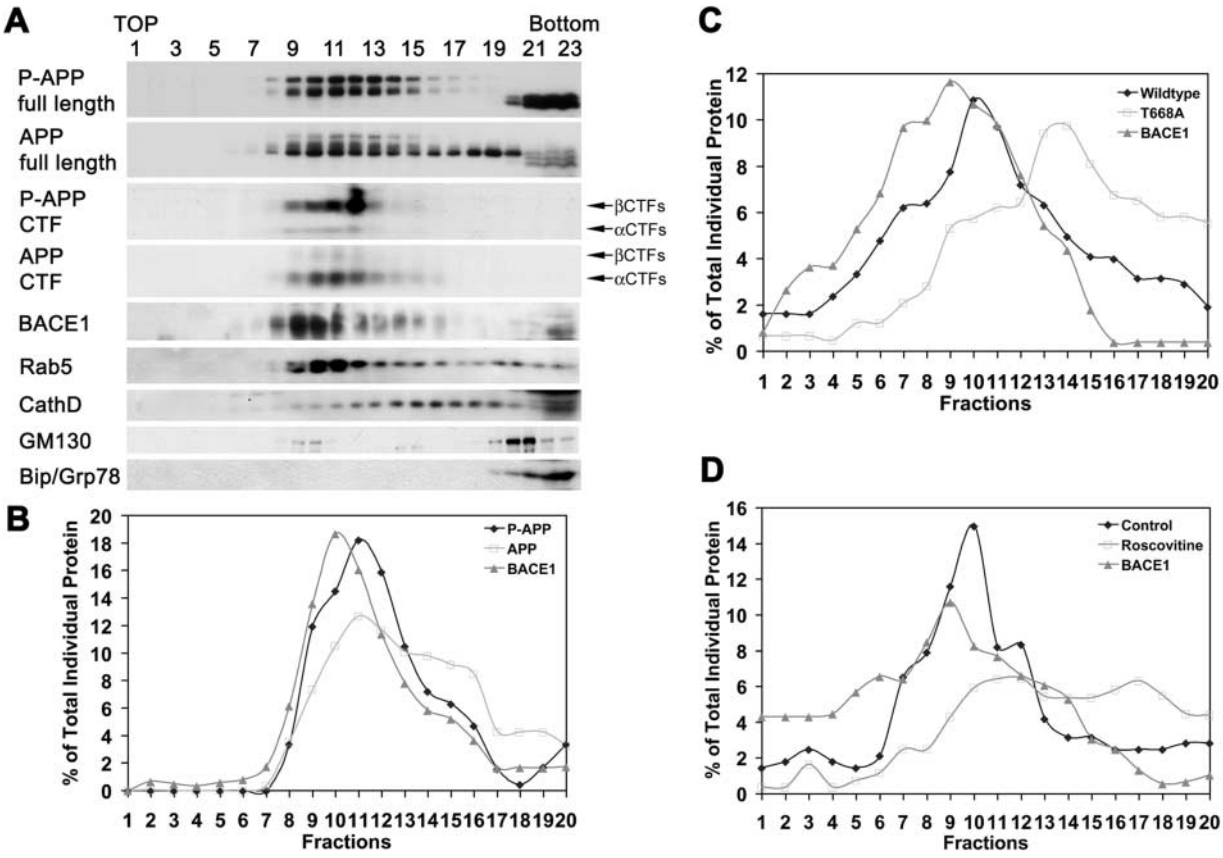

Figure 6. **T668 phosphorylated APP cofractionates with BACE1 and endosome markers.** (A) Adult mouse brain homogenates were fractionated through an iodixanol step gradient. Western blot analysis showed the distribution of P-APP, APP, Rab5 (early endosome marker), cathepsin D (lysosome marker), GM130 (Golgi marker), Bip (ER marker), and BACE1. (B) Quantification of protein distribution of A (fractions 1–20), showing that full-length P-APP largely cofractionates with BACE1. (C) Distribution of wild-type and T668A mutant APP, expressed in rat primary cortical neurons using recombinant HSV in an iodixanol step gradient. Note that the distribution pattern of BACE1 resembles that of wild-type APP. (D) Distribution of wild-type APP in an iodixanol step gradient after roscovitine treatment (15 μM for 8 h). APP distribution shifted to heavier membrane fractions after roscovitine treatment.

full/jcb.200301115/DC1). T668 of APP can be phosphorylated by multiple kinases including Cdc2 and Cdk5. The activities of these Cdks can be inhibited by pharmacological reagents roscovitine and butyrolactone. We analyzed APP distribution from roscovitine treated cortical neurons by fractionation using iodixanol gradient. Similarly, we found that APP distribution shifted to heavier membrane fractions after roscovitine treatment (Fig. 6 D; immunoblots in Fig. S6 B). This observation indicates that T668 phosphorylation plays a role in the intracellular trafficking of APP.

APP CTFs generated by β-secretase are preferentially phosphorylated on T668

To further determine the species of APP CTFs that is phosphorylated on T668 in vivo, we performed immunodepletion experiments. We used CTFs derived from CAD cells overexpressing C99, a β-secretase products of APP, as markers for identifying different CTF species (Fig. 7, A and B, lane 1). We found that CTFs from mouse brain lysates generally showed slower mobility than those from C99 overexpressing CAD cells, possibly due to differences in the stoichiometry of phosphorylation. As such, we assigned those CTFs with slower mobility than C99 from CAD cells as βCTFs and those with faster mobility than C89 as αCTFs. In these brain lysates, αCTFs were much more abundant than βCTFs (Fig. 7, A and B, bottom). Increasing amounts of αP-T668 efficiently immunoprecipitated βCTFs, as recognized by the APP COOH-terminal antibody, in a dose-dependent manner (Fig. 7 A, top). A corresponding dose-dependent decrease in βCTFs was observed in the supernatant of these immunoprecipitates (Fig. 7 A, bottom). On the other hand, the level of αCTFs in the supernatants only decreased slightly. When 10 μg of αP-T668 was used, ~60% of βCTFs were depleted, whereas only <10% of αCTFs were depleted from the brain lysates (Fig. 7 C). As a control, we used the APP COOH-terminal antibody to immunoprecipitate APP CTFs from mouse brain lysates. This antibody efficiently removed both αCTFs and βCTFs from the lysates (Fig. 7, B and C). These observations suggest that the β-secretase products of APP are preferentially phosphorylated on T668 in vivo and raise the possibility that T668 phosphorylation may facilitate APP cleavage by BACE1.

Effects of T668 phosphorylation on Aβ generation in primary cortical neurons

To elucidate whether T668 phosphorylation plays a role in Aβ generation, we assessed Aβ levels from the cultured media of neurons treated with the Cdk inhibitors roscovitine or bu-

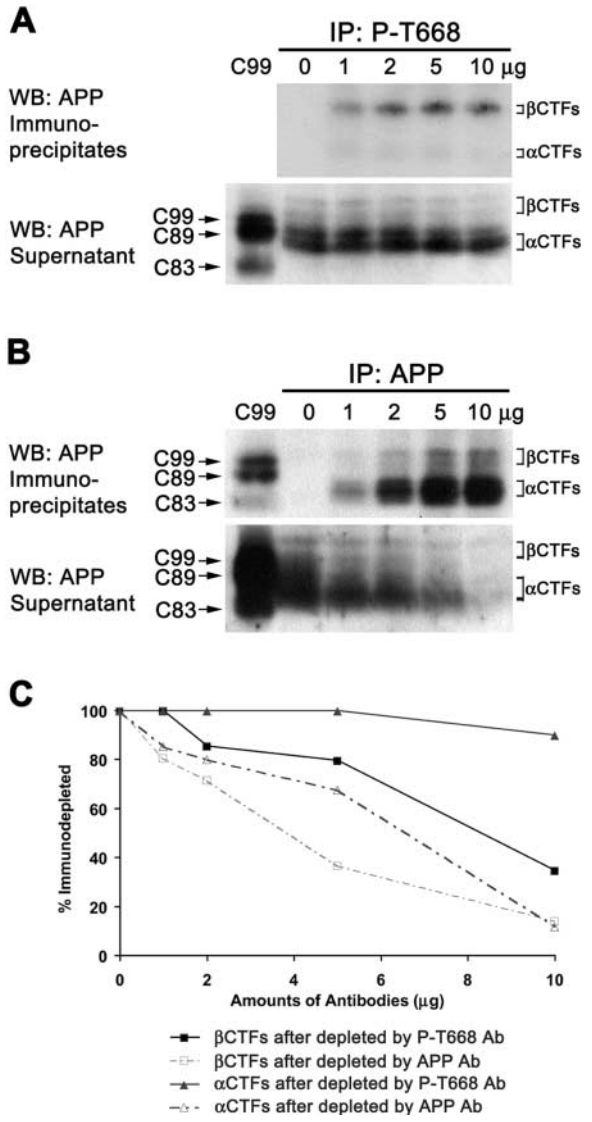

Figure 7. **βCTFs are preferentially phosphorylated on T668.** (A) Increasing amounts of αP-T668 was used to immunoprecipitate APP from lysates prepared from a 6-mo-old mouse brain. Western blot analysis using a pan APP antibody (C1/6.1) showed that increasing levels of βCTFs were efficiently precipitated by αP-T668, whereas little αCTFs were brought down by αP-T668 (top). Conversely, in the supernatants, a dose-dependent decrease of βCTFs but not αCTFs was observed. (B) The C1/6.1 antibody efficiently immunoprecipitated both βCTFs and αCTFs. In supernatants, both βCTFs and αCTFs were completely removed using 10 µg of C1/6.1 antibody. (C) Quantification of the levels of βCTFs and αCTFs in supernatants from A and B reveals that βCTFs are efficiently removed from the brain lysates by αP-T668.

tyrolactone. Because the levels of secreted Aβ from endogenous APP was too low to be detected, we used recombinant HSV to express wild-type APP in rat cortical neurons. Both roscovitine and butyrolactone treatments caused substantial decreases in T668 phosphorylation (Fig. 8 B). Interestingly, levels of secreted Aβ 1-40 and 1-42 were significantly reduced by these inhibitors in a dose-dependent manner (Fig. 8 A). The reduction in Aβ secretion was not due to a decline in cell viability as determined by the MTT assay (unpublished data).

Butyrolactone and roscovitine are general Cdk inhibitors. Because Cdks phosphorylate many substrates, it is possible that the reduction in Aβ secretion is an indirect effect resulting from reduced phosphorylation of proteins other than APP. To directly test the hypothesis that T668 phosphorylation is involved in the metabolism of APP, we compared Aβ levels generated from neurons expressing wild-type versus T668A mutant APP. Rat cortical neurons 2 d in vitro were infected with HSV expressing either wild-type or the T668A mutant APP. The Aβ levels in the culture media were determined 20 h after infection. Fig. 8 D showed that the expression levels of wild-type and T668A mutant APP were comparable in these cultures. However, Aβ 1-40 and 1-42 levels in neuronal cultures expressing the T668A mutant APP were significantly reduced compared with those expressing wild-type APP (Fig. 8 C). These results suggest that phosphorylation of T668 regulates APP processing and Aβ generation.

Discussion

T668 of APP has been shown to be phosphorylated in cells undergoing mitosis and in cultured cortical neurons (Suzuki et al., 1994; Iijima et al., 2000). Here, we show that phosphorylation of T668 is elevated in AD brain samples. In AD brain sections, we observed the most prominent P-APP signals in hippocampus. P-APP signal is associated with dystrophic neurites surrounding the plaques, and with enlarged endosomes primarily in the soma of hippocampal neurons. In addition, we found that most of the neurons exhibiting P-APP–positive vesicles in the soma are also positive for AT8 staining, an antibody specific for phospho-Tau. Therefore, elevation of P-APP is specifically present in the neuronal population afflicted in AD. We have also surveyed human brain samples of other neurodegenerative diseases including Huntington's disease, Parkinson's disease, Progressive Supranuclear Palsy and Frontal Temporal Dementia, and have not found significant vesicular staining of P-APP (unpublished data). These observations suggest that the enrichment of the T668 phosphorylated APP in the enlarged endosomes is a pathology specific to AD.

P-APP and BACE1 signals are enriched in enlarged endosomes in AD brains

It has been recently reported that the expression levels and activities of BACE1 are up-regulated in AD brains, especially in neurons of temporal cortex and hippocampus (Fukumoto et al., 2002; Holsinger et al., 2002). Interestingly, we found that BACE1 signal is enriched in the enlarged endosomes of hippocampal pyramidal neurons in AD brain sections. Furthermore, BACE1 colocalizes with P-APP in these enlarged endosomes. Analysis of AD brain lysates reveals that phosphorylation of APP CTFs on T668 is up-regulated. In addition, we also found that the βCTFs are preferentially phosphorylated on T668. Together, these observations suggest that P-APP is preferentially cleaved by the increased BACE1 in AD brain, possibly in the endosomes. Enhanced endocytic activity is one of the earliest known neuropathological alternations in sporadic Alzheimer's disease. Abnormalities associated with the endocytic pathway have been proposed to play a role in Aβ genera-

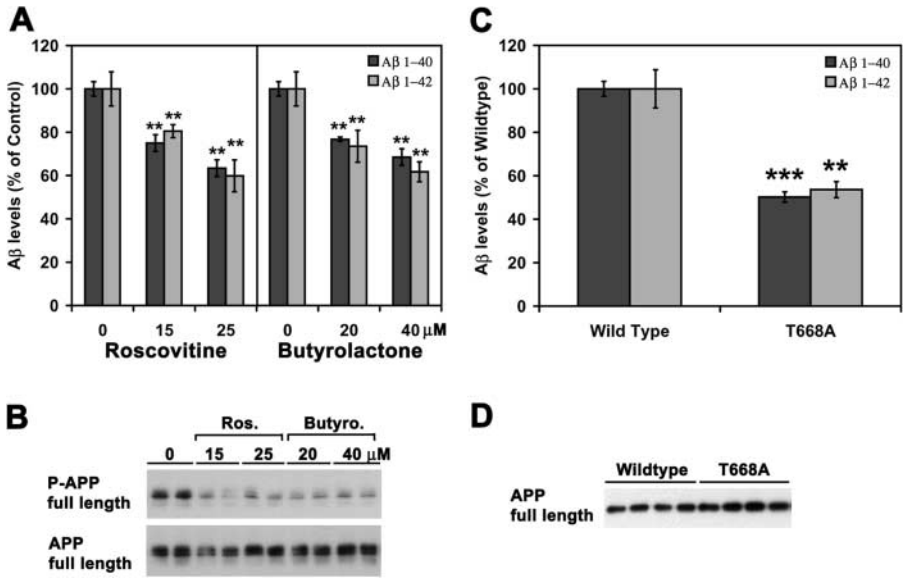

Figure 8. **Reduced Aβ generation by APP T668 to alanine mutant and T668 kinase inhibitors in primary cortical neurons.** (A) Inhibiting T668 phosphorylation by Cdk inhibitors leads to a decrease in Aβ secretion. Rat primary cortical neurons were treated with recombinant HSV expressing wild-type APP for 16 h and subsequently with indicated concentrations of roscovitine or butyrolactone for 8 h. The levels of secreted Aβ 1-40 or Aβ 1-42 were measured by sandwich ELISA and data were normalized against the untreated control. The data shown represent the average (±SEM) of three independent experiments. (**$P < 0.01$; $P = 0.0051$ for Aβ 1-40 and $P = 0.0071$ for Aβ 1-42 under roscovitine treatment; and $P = 0.0054$ for Aβ 1-40 and $P = 0.0087$ for Aβ 1-42 under butyrolactone treatment). (B) T668 phosphorylation levels of full-length APP were detected by Western blot of cell lysates. (C) Aβ generation from rat primary cortical neurons expressing recombinant wild-type or T668A APP. Levels of Aβ 1-40 and Aβ 1-42 secreted into the media from virus infected cultures were measured by sandwich ELISA. Markedly reduced Aβ 1-40 and Aβ 1-42 were detected from neurons expressing the APP T668A mutant compared to those expressing wild-type APP. The data shown represent the average (±SEM) of three independent experiments with quadruple infections in each experiment. (** $P < 0.01$ and *** $P < 0.001$; and $P < 0.0001$ for Aβ 1-40 and $P = 0.0027$ for Aβ 1-42). (D) Western blot analysis from four independent infections showed that the expression level of full-length APP was comparable between wild-type and T668A mutant APP.

tion (Cataldo et al., 2000; Nixon et al., 2000). Recent studies by Grbovic et al. (2003) demonstrated that Aβ generation could be up-regulated by enhanced endocytic activity as a result of overexpression of Rab5. As such, the drastic up-regulation and accumulation of BACE1 and P-APP in the endocytic vesicles implies the significance of the enlarged endosomes in contributing to the altered processing of APP in AD.

P-APP is preferentially associated with BACE1 in the endocytic pathway in primary cortical neurons

Endocytic pathway is one of the major sites where Aβ is normally generated (Nordstedt et al., 1993; Koo and Squazzo, 1994). The presence of APP in the Rab5-positive endocytic compartments has been shown previously in rat brain nerve terminals (Ikin et al., 1996). Here, we found that P-APP is present in Rab5 labeled endocytic vesicles and exhibits extensive colocalization with BACE1 in growth cones of young cortical neurons. This observation is further supported by the coimmunoisolation of Rab5 with P-APP– and BACE1-positive vesicles. In addition, P-APP and BACE1 cosegregate in the iodixanol gradient. In the gradient, the fractionation profiles of P-APP and BACE1 largely overlap with Rab5. As for older neurons, the colocalization of P-APP and BACE1 is less prominent. Although endosomes are highly enriched in the growth cones of young neurons, endosomes of mature neurons are concentrated in branch region of axons and presynaptic nerve terminals (Overly and Hollenbeck, 1996). Studies by Sabo et al. showed that APP is localized in Rab5 containing synaptic organelles in mature neurons (Sabo et al., 2003). It is possible that P-APP and BACE1 colocalize in specific loci of neurites, such as areas where synapses form in mature neurons.

Unlike the staining pattern of AD brains, we detected modest colocalization of P-APP with the early endosome marker EEA1, in primary cortical neurons. In the early endocytic pathway, Rab5 regulates both clathrin-coated vesicle-mediated transport from the plasma membrane to the early endosomes, as well as homotypic early endosome fusion, whereas EEA1 medicates homotypic early endosome fusion. Our findings suggest that in normal conditions, P-APP is localized in Rab5-positive endocytic vesicles that do not actively undergo homotypic endosome fusion. In addition, we did not observe extensive colocalization of P-APP with recycling endosome marker Rab4 in primary cortical neurons. It is likely that the colocalization of P-APP and EEA1/Rab4 in AD brains is due to abnormalities in endocytic pathway associated with the disease state. We detected little colocalization of P-APP with the TGN marker adaptin-γ and the cis-Golgi marker GM130. These observations suggest that P-APP is preferentially exposed to BACE1 in the Rab5-positive endosomes. Although BACE1 cleaves APP in both the secretory pathway and endocytic compartments, our results suggest that T668 phosphorylated APP is likely the target of BACE1 in the Rab5-positive endocytic compartments in both normal and disease conditions.

T668 phosphorylation regulates APP processing

A contribution of T668 phosphorylation on APP processing is underscored by the significantly reduced Aβ 1-40 and 1-42 secretion from neurons treated with T668 kinase inhibitors or neurons expressing the T668A mutant APP. In normal mouse brain lysates, the αCTF is much more abundant than the βCTFs. Interestingly, αP-T668 preferentially recognizes βCTFs over αCTF and efficiently depletes βCTFs from the brain lysates. This observation strongly suggests

that P-APP is more likely to be cleaved by the β-secretase. Whether T668 phosphorylation of APP directly or indirectly impacts on BACE1 cleavage remains to be determined.

We found that the T668A mutant produces 50% less Aβ compared with the wild-type APP in cultured neurons. This observation indicates that in the absence of T668 phosphorylation, Aβ is still generated, albeit less efficiently. Therefore, it is less likely that T668 phosphorylation directly impacts on APP cleavage. Rather, T668 phosphorylation is likely to be involved in the intracellular sorting and trafficking of APP, which in turn impacts on the proteolytic cleavage of APP. This view is supported by the observation that the T668A mutant is mislocalized as evident by its distribution in the heavier fractions of iodixanol gradient.

Previous studies by Ando et al. (2001) reported that T668 glutamate mutant of APP (T668E) did not affect Aβ generation in HEK293 cells. Unlike the T668E mutant, expression of the T668A mutant causes mislocalization of APP and a decrease in Aβ generation. This, together with the observation that Cdk inhibitors roscovitine and butyrolactone elicit the same effect as T668A mutant, strongly argues that T668 phosphorylation of APP plays a role in regulating trafficking of APP and Aβ generation.

From solution NMR studies, it has been predicted that phosphorylation of T668 may result in a dramatic conformational change of the APP cytoplasmic tail, which is likely to affect the interaction of APP with its binding partners. Indeed, Ando and colleagues showed that T668 phosphorylation weakens the interaction of APP with Fe65 (Ando et al., 2001). However, the impact of the interactions of APP with Fe65 on the metabolism of APP is less clear. Guenette et al. (1996) and Sabo et al. (1999) reported that expressing Fe65 in MDCK and H4 neuroglioma cells lead to increased accumulation of APP on the cell surface and increased secretion of Aβ. On the contrary, overexpression of Fe65 resulted in reduced Aβ secretion in HEK293 cells (Ando et al., 2001). As such, the effect of Fe65 appears to be cell-type specific. It is possible that disruption of the APP–Fe65 interaction through phosphorylation of T668 represents one of the mechanisms underlying increased generation of Aβ.

When considered together, our findings that T668 phosphorylation facilitates APP and BACE1 colocalization and that inhibition of T668 phosphorylation decreases Aβ generation suggest that T668 phosphorylation of APP is a molecular mechanism regulating its cleavage by BACE1. As BACE1 cleavage is the essential step for Aβ generation, understanding how proteolysis by BACE1 is regulated will help elucidate the intricate intracellular signaling network regulating the generation of Aβ.

Materials and methods

DNA constructs

GST fusion protein of cytoplasmic domain of APP (residues 649–695) was constructed by PCR and cloned into the bacterial expression vector pGEX-4T2 (Amersham Biosciences). The APP T668A and T668E constructs were generated via PCR using complementary primers as described previously (Niethammer et al., 2000).

Antibodies

Anti-APP (C1/6.1) was a gift from R.A. Nixon and P.M. Mathews (both from Nathan Kline Institute, Orangeburg, NY). 4G8 was obtained from Senetek. AT8 was obtained from Innogenetics. Anti-BACE1 was obtained from Oncogene Research Products and Calbiochem. Anti-Rab5 and anti-Bip were obtained from StressGen Biotechnologies. Anti-Rab4, anti-Rab7, and anti–cathepsin D were obtained from Santa Cruz Biotechnology, Inc. Anti–adaptin-γ and anti-GM130 were obtained from BD Biosciences. Anti-PS1 mAbs and pAbs were obtained from CHEMICON International, Inc. and a gift from D. Selkoe (Harvard Medical School). Anti-SV2 and anti–cathepsin β were gifts from K.M. Buckley and H.L. Ploegh, respectively (both from Harvard Medical School).

Generation of αP-T668

The phospho-epitope–specific APP antibody was generated against a synthetic peptide antigen corresponding to APP phosphorylated at the T668 residue: VDAAVpTPEERHC, where *p*T denotes phosphothreonine (Tufts Peptide Synthesis Core Facility). The peptide was conjugated to KLH with sulfo-MBS (Pierce Chemical Co.) and injected into NZW rabbits (Covance Research Products Inc.). The antiserum was first adsorbed against a corresponding nonphosphorylated peptide, VDAAVTPEERHC, and purified with the phospho-peptide coupled to a SulfoLink coupling column (Pierce Chemical Co.).

Cell line and neuronal cell culture

Catecholaminergic cell lines (CAD cells) were cultured in DME supplemented with 10% FBS and L-glutamine in a humidified 5% CO_2 incubator.

Primary cultures of embryonic rat cortical neurons were prepared as described previously (Niethammer et al., 2000). In brief, dissociated embryonic neurons from E18 Sprague-Dawley pregnant rats were plated onto poly-D-lysine/laminin–coated 24-well plates or coverslips and maintained in neurobasal medium (Invitrogen) supplemented with B27 (Invitrogen), L-glutamine (Sigma-Aldrich) and 1% penicillin-streptomycin sulfate.

Generation of recombinant HSV

Wild-type and T668A APP coding sequence were subcloned into a replication-defective HSV vector pHSVPrpUC. The resultant recombinant plasmid was packaged into virus particles in the packaging line 2–2 using the protocol described previously (Lim et al., 1996). The virus was then purified on a sucrose gradient, pelleted, and resuspended in 10% sucrose and the titer of the recombinant virus was determined.

Immunohistochemistry

AD and control tissues were obtained from the autopsy service at Brigham and Women's Hospital. Neuropathological diagnosis of AD was confirmed according to the criteria of Khachaturian (1985). Blocks of AD or control hippocampi were fixed (1–48 h) in 10% neutral buffered formalin. After fixation, the brain tissue was dehydrated and embedded in paraffin. 20 micrometer serial sections were cut, dried, and baked at 60°C for 1 h. Serial sections were immunostained using the avidin-biotin HFP/DAB method (Vector Laboratories) or by immunofluorescence. Details of the immunostaining protocol have been described previously (Lemere et al., 1996). All images were captured using an inverted microscope (Nikon) linked to a DeltaVision deconvolution imaging system (Applied Biosystems). For some immunofluorescence staining, the primary antibody was directly labeled with Oregon green using the FluoReporter Oregon green 488 protein labeling kit (Molecular Probes) according to manufacturer's specifications.

For the peptide preadsorption experiment, antibodies were mixed with peptides at a 1:100 molar ratio and incubated overnight at 4°C before being used for staining.

Immunocytochemistry

Primary cortical neurons from E18 rat embryos were cultured at a density of 10^5 cells/well in 24-well plates. 2 d after plating, neurons were fixed in 4% PFA for 30 min, blocked, and permeabilized in 10% normal goat serum and 0.1% Triton in PBS for 20 min. Permeabilized neurons were incubated with primary antibodies for 1 h at room temperature, and subsequently incubated with Oregon green– or Texas red–conjugated secondary antibodies (Molecular Probes). Images were captured using an inverted microscope (Nikon) linked to a DeltaVision deconvolution imaging system (Applied Biosystems).

Immunodepletion

Immunodepletion was performed by lysing the mouse brain in RIPA buffer (50 mM Tris, pH 8.0, 1% NP-40, 0.5% sodium deoxycholate, 0.1% SDS, 150 mM NaCl, and protease and phosphatase inhibitors [1 mM PMSF, 1 μg/ml aprotinin and leupeptin, and 20 mM β-glycerol phosphate]) using a Dounce homogenizer. The lysates were centrifuged at 13,000 rpm for 15

min at 4°C. 300 μg of lysates were incubated with indicated amounts of antibodies and 30 μl of 50% slurry of protein A–Sepharose (Amersham Biosciences) at 4°C for 2.5 h. The immunoprecipitates were washed three times with RIPA buffer, resuspended in Laemmli sample buffer, and analyzed by Western blot analysis.

Immunoisolation

Adult mouse brain was homogenized in 2 ml of immunoisolation buffer (250 mM sucrose, 20 mM Hepes, pH 7.3, 5 mM $MgCl_2$, and protease and phosphatase inhibitors) by 20 strokes in a Dounce homogenizer followed by an additional 20 strokes in a 1-ml syringe fitted with 21-gauge needle. Lysates were centrifuged at 3,000 rpm for 15 min. The postnuclear supernatant (PNS) was collected and centrifuged at 27,000 rpm for 30 min to precipitate vesicles. The resulting pellet was resuspended in immunoisolation buffer that did not contain sucrose. Equal amounts of vesicle suspension were incubated at 4°C overnight with indicated antibody that had been preconjugated to M-280 Tosylactivated Dynabeads (Dynal) according to the manufacturer's instructions. Immunoisolates were washed three times with immunoisolation buffer containing 0.1% BSA, resuspended in Laemmli sample buffer, and subjected to Western blot analysis.

Mass spectrometric analysis

Blocks of AD hippocampi (gifts from M. Frosch, Massachusetts General Hospital, Boston, MA) were lysed in RIPA buffer using a Dounce homogenizer. T668 phosphorylated APP were isolated using a αP-T668 column according to the manufacturer's instructions (Amersham Biosciences). Isolated proteins were resolved using SDS-PAGE. Protein bands containing APP-CTFs were cut and subjected to S-carbamidomethylation and in-gel trypsin digestion (Stensballe and Jensen, 2001). Peptide digests were extracted in 25 mM ammonium bicarbonate, pH 8.8, containing 25% (vol/vol) dimethyl foramide and further purified using ZipTipC18 (Millipore). Purified peptides were mixed with α–cyano-4-hydroxycinnamic acid matrix and analyzed by Voyager DE-STR mass spectrometer (PerSeptive Biosystems). Postsource decay experiments were performed according to the protocols provided the manufacturer. Tables of mass/charge (m/z) of trypsinized APP peptides were generated using Protein Prospector (http://prospector.ucsf.edu/). The tolerance of the difference between experimental and theoretical m/z values in comparison was constrained under 300 ppm.

Iodixonal step gradient

Half of a 1-mo-old adult mouse brain was homogenized in 1 ml of homogenization buffer (HB: 250 mM sucrose, 20 mM Tris-HCl, pH 7.4, 1 mM EGTA, 1 mM EDTA, and protease and phosphatase inhibitors) by 20 strokes in a Dounce homogenizer followed by an additional 20 strokes in a 1-ml syringe fitted with 21-gauge needle. Lysates were centrifuged at 3,000 rpm for 15 min to generate the PNS. The PNS was then adjusted to 25% OptiPrep (Nycomed/Axis-Shield PoC.) with 50% OptiPrep in HB. The resulting mixture, 2 ml in 25% OptiPrep, was placed at the bottom of an ultracentrifuge tube (14 × 89 mm) and was overlaid successively with 1 ml each of 20, 18.5, 16.5, 14.5, 12.5, 10.5, 8.5, 6.5, and 5% OptiPrep in cold HB. The gradients were centrifuged for 20 h at 27,000 rpm at 4°C in a rotor (model SW41; Beckman Coulter). 500μl fractions were collected from the top of the ultracentrifuge tubes and analyzed by Western blot analysis. P-APP, APP, and BACE levels in each fraction were digitized by a Luminescent Image Analyzer (Fujifilm) and expressed as a percentage of the sum of all of the fractions.

Aβ measurement by ELISA assay

T668 kinase inhibitor. Primary cortical neurons were cultured from E18 rat embryos at a density of 4×10^5 cells/well in 24-well plates. 2 d after plating, neurons were infected with recombinant HSV expressing wild-type APP for 16 h. Subsequently, 70% of culture media was replaced with fresh medium and neurons were treated with indicated concentration of Roscovitine or Butyrolactone. 8 h after inhibitor treatment, culture media was collected and subjected to sandwich ELISA assay according to the manufacturer's specifications (Biosource International).

T668A mutant. Primary cortical neurons from E18 rat embryos were cultured at a density of 2×10^5 cells/well in 24-well plates. 2 d after plating, 70% of culture media was replaced with fresh medium. Neurons were subsequently infected with equal titer of HSV expressing either wild-type or T668A APP. 20 h after infection, culture media was collected and subjected to sandwich ELISA assay. We observed most dramatic effect on Aβ generation 24 h after infection. By 48 h after infection, the effect is less pronounced. Data were analyzed by *t* test using Prism (GraphPad). Differences were considered significant at $P < 0.05$.

Online supplemental material

The supplemental material (Figs. S1–S6 and Tables S1 and S2) is available at http://www.jcb.org/cgi/content/full/jcb.200301115/DC1. Fig. S1 shows characterization of αP-T668. Fig. S2 shows additional controls for αP-T668 staining of AD brain sections and that αP-T668 labels dystrophic neurites closely associated with amyloid plaques in APPswe Tg mice. Fig. S3 shows a partial MALDI-TOF MS spectrum of APP CTFs from CAD cells overexpressing human APP. Figs. S4 and S5 show costaining of P-APP and organelle markers in AD brain sections and in rat primary cortical neurons. Fig S6 shows distribution of wild-type, T668A mutant APP, and BACE1 from cultured cortical neurons in iodixanol step gradient. Tables S1 and S2 show case information of human brains analyzed by immunohistochemistry and Western blot analysis.

We would like to thank Dr. D.M. Walsh for discussion and critical reading of the manuscript and Drs. L. Moy, B.A. Samuels, H. Patzke, J. Cruz, Z. Xie, and other members of the Tsai lab for comments on the manuscript.

This project was partially supported by MetLife Foundation Award made to L.-H. Tsai. L.-H. Tsai is an Associate Investigator of the Howard Hughes Medical Institute.

Submitted: 28 January 2003
Accepted: 11 August 2003

References

Ando, K., K.I. Iijima, J.I. Elliott, Y. Kirino, and T. Suzuki. 2001. Phosphorylation-dependent regulation of the interaction of amyloid precursor protein with Fe65 affects the production of beta-amyloid. *J. Biol. Chem.* 276: 40353–40361.

Annaert, W.G., L. Levesque, K. Craessaerts, I. Dierinck, G. Snellings, D. Westaway, P.S. George-Hyslop, B. Cordell, P. Fraser, and B. De Strooper. 1999. Presenilin 1 controls γ-secretase processing of amyloid precursor protein in pre-Golgi compartments of hippocampal neurons. *J. Cell Biol.* 147:277–294.

Aplin, A.E., G.M. Gibb, J.S. Jacobsen, J.M. Gallo, and B.H. Anderton. 1996. In vitro phosphorylation of the cytoplasmic domain of the amyloid precursor protein by glycogen synthase kinase-3beta. *J. Neurochem.* 67:699–707.

Cataldo, A.M., C.M. Peterhoff, J.C. Troncoso, T. Gomez-Isla, B.T. Hyman, and R.A. Nixon. 2000. Endocytic pathway abnormalities precede amyloid beta deposition in sporadic Alzheimer's disease and Down syndrome: differential effects of APOE genotype and presenilin mutations. *Am. J. Pathol.* 157: 277–286.

De Strooper, B., and W. Annaert. 2000. Proteolytic processing and cell biological functions of the amyloid precursor protein. *J. Cell Sci.* 113:1857–1870.

De Strooper, B., M. Beullens, B. Contreras, L. Levesque, K. Craessaerts, B. Cordell, D. Moechars, M. Bollen, P. Fraser, P.S. George-Hyslop, and F. Van Leuven. 1997. Phosphorylation, subcellular localization, and membrane orientation of the Alzheimer's disease-associated presenilins. *J. Biol. Chem.* 272: 3590–3598.

Fukumoto, H., B.S. Cheung, B.T. Hyman, and M.C. Irizarry. 2002. Beta-secretase protein and activity are increased in the neocortex in Alzheimer disease. *Arch. Neurol.* 59:1381–1389.

Grbovic, O.M., P.M. Mathews, Y. Jiang, S.D. Schmidt, R. Dinakar, N.B. Summers-Terio, B.P. Ceresa, R.A. Nixon, and A.M. Cataldo. 2003. Rab5-stimulated up-regulation of the endocytic pathway increases intracellular levels of beta-cleaved amyloid precursor protein carboxyl-terminal fragment levels and Abeta production. *J. Biol. Chem.* 278:31261–31268.

Guenette, S.Y., J. Chen, P.D. Jondro, and R.E. Tanzi. 1996. Association of a novel human FE65-like protein with the cytoplasmic domain of the beta-amyloid precursor protein. *Proc. Natl. Acad. Sci. USA.* 93:10832–10837.

Hardy, J., and R. Crook. 2001. Presenilin mutations line up along transmembrane alpha-helices. *Neurosci. Lett.* 306:203–205.

Holsinger, R.M., C.A. McLean, K. Beyreuther, C.L. Masters, and G. Evin. 2002. Increased expression of the amyloid precursor beta-secretase in Alzheimer's disease. *Ann. Neurol.* 51:783–786.

Iijima, K., K. Ando, S. Takeda, Y. Satoh, T. Seki, S. Itohara, P. Greengard, Y. Kirino, A.C. Nairn, and T. Suzuki. 2000. Neuron-specific phosphorylation of Alzheimer's beta-amyloid precursor protein by cyclin-dependent kinase 5. *J. Neurochem.* 75:1085–1091.

Ikin, A.F., W.G. Annaert, K. Takei, P. De Camilli, R. Jahn, P. Greengard, and J.D. Buxbaum. 1996. Alzheimer amyloid protein precursor is localized in nerve terminal preparations to Rab5-containing vesicular organelles distinct from those implicated in the synaptic vesicle pathway. *J. Biol. Chem.* 271:

31783–31786.

Khachaturian, Z.S. 1985. Diagnosis of Alzheimer's disease. *Arch. Neurol.* 42: 1097–1105.

Koo, E.H., and S.L. Squazzo. 1994. Evidence that production and release of amyloid beta-protein involves the endocytic pathway. *J. Biol. Chem.* 269: 17386–17389.

Kovacs, D.M., H.J. Fausett, K.J. Page, T.W. Kim, R.D. Moir, D.E. Merriam, R.D. Hollister, O.G. Hallmark, R. Mancini, K.M. Felsenstein, et al. 1996. Alzheimer-associated presenilins 1 and 2: neuronal expression in brain and localization to intracellular membranes in mammalian cells. *Nat. Med.* 2:224–229.

Lah, J.J., and A.I. Levey. 2000. Endogenous presenilin-1 targets to endocytic rather than biosynthetic compartments. *Mol. Cell. Neurosci.* 16:111–126.

Lai, A., A. Gibson, C.R. Hopkins, and I.S. Trowbridge. 1998. Signal-dependent trafficking of beta-amyloid precursor protein-transferrin receptor chimeras in madin-darby canine kidney cells. *J. Biol. Chem.* 273:3732–3739.

Lemere, C.A., J.K. Blusztajn, H. Yamaguchi, T. Wisniewski, T.C. Saido, and D.J. Selkoe. 1996. Sequence of deposition of heterogeneous amyloid beta-peptides and APO E in Down syndrome: implications for initial events in amyloid plaque formation. *Neurobiol. Dis.* 3:16–32.

Lim, F., D. Hartley, P. Starr, P. Lang, S. Song, L. Yu, Y. Wang, and A.I. Geller. 1996. Generation of high-titer defective HSV-1 vectors using an IE 2 deletion mutant and quantitative study of expression in cultured cortical cells. *Biotechniques.* 20:460–469.

Niethammer, M., D.S. Smith, R. Ayala, J. Peng, J. Ko, M.S. Lee, M. Morabito, and L.H. Tsai. 2000. NUDEL is a novel Cdk5 substrate that associates with LIS1 and cytoplasmic dynein. *Neuron.* 28:697–711.

Nixon, R.A., A.M. Cataldo, and P.M. Mathews. 2000. The endosomal-lysosomal system of neurons in Alzheimer's disease pathogenesis: a review. *Neurochem. Res.* 25:1161–1172.

Nordstedt, C., G.L. Caporaso, J. Thyberg, S.E. Gandy, and P. Greengard. 1993. Identification of the Alzheimer beta/A4 amyloid precursor protein in clathrin-coated vesicles purified from PC12 cells. *J. Biol. Chem.* 268:608–612.

Oishi, M., A.C. Nairn, A.J. Czernik, G.S. Lim, T. Isohara, S.E. Gandy, P. Greengard, and T. Suzuki. 1997. The cytoplasmic domain of Alzheimer's amyloid precursor protein is phosphorylated at Thr654, Ser655, and Thr668 in adult rat brain and cultured cells. *Mol. Med.* 3:111–123.

Overly, C.C., and P.J. Hollenbeck. 1996. Dynamic organization of endocytic pathways in axons of cultured sympathetic neurons. *J. Neurosci.* 16:6056–6064.

Perez, R.G., S. Soriano, J.D. Hayes, B. Ostaszewski, W. Xia, D.J. Selkoe, X. Chen, G.B. Stokin, and E.H. Koo. 1999. Mutagenesis identifies new signals for beta-amyloid precursor protein endocytosis, turnover, and the generation of secreted fragments, including Abeta42. *J. Biol. Chem.* 274:18851–18856.

Price, D.L., S.S. Sisodia, and S.E. Gandy. 1995. Amyloid beta amyloidosis in Alzheimer's disease. *Curr. Opin. Neurol.* 8:268–274.

Ramelot, T.A., and L.K. Nicholson. 2001. Phosphorylation-induced structural changes in the amyloid precursor protein cytoplasmic tail detected by NMR. *J. Mol. Biol.* 307:871–884.

Sabo, S.L., L.M. Lanier, A.F. Ikin, O. Khorkova, S. Sahasrabudhe, P. Greengard, and J.D. Buxbaum. 1999. Regulation of beta-amyloid secretion by FE65, an amyloid protein precursor-binding protein. *J. Biol. Chem.* 274:7952–7957.

Sabo, S.L., A.F. Ikin, J.D. Buxbaum, and P. Greengard. 2003. The amyloid precursor protein and its regulatory protein, FE65, in growth cones and synapses in vitro and in vivo. *J. Neurosci.* 23:5407–5415.

Selkoe, D.J., T. Yamazaki, M. Citron, M.B. Podlisny, E.H. Koo, D.B. Teplow, and C. Haass. 1996. The role of APP processing and trafficking pathways in the formation of amyloid beta-protein. *Ann. NY Acad. Sci.* 777:57–64.

Sinha, S., J.P. Anderson, R. Barbour, G.S. Basi, R. Caccavello, D. Davis, M. Doan, H.F. Dovey, N. Frigon, J. Hong, et al. 1999. Purification and cloning of amyloid precursor protein beta-secretase from human brain. *Nature.* 402: 537–540.

Standen, C.L., J. Brownlees, A.J. Grierson, S. Kesavapany, K.F. Lau, D.M. McLoughlin, and C.C. Miller. 2001. Phosphorylation of thr(668) in the cytoplasmic domain of the Alzheimer's disease amyloid precursor protein by stress-activated protein kinase 1b (Jun N-terminal kinase-3). *J. Neurochem.* 76:316–320.

Steiner, H., and C. Haass. 2000. Intramembrane proteolysis by presenilins. *Nat. Rev. Mol. Cell Biol.* 1:217–224.

Steinhilb, M.L., R.S. Turner, and J.R. Gaut. 2002. ELISA analysis of beta-secretase cleavage of the Swedish amyloid precursor protein in the secretory and endocytic pathways. *J. Neurochem.* 80:1019–1028.

Stensballe, A., and O.N. Jensen. 2001. Simplified sample preparation method for protein identification by matrix-assisted laser desorption/ionization mass spectrometry: in-gel digestion on the probe surface. *Proteomics.* 1:955–966.

Suzuki, T., M. Oishi, D.R. Marshak, A.J. Czernik, A.C. Nairn, and P. Greengard. 1994. Cell cycle-dependent regulation of the phosphorylation and metabolism of the Alzheimer amyloid precursor protein. *EMBO J.* 13:1114–1122.

Tarr, P.E., R. Roncarati, G. Pelicci, P.G. Pelicci, and L. D'Adamio. 2002. Tyrosine phosphorylation of the beta-amyloid precursor protein cytoplasmic tail promotes interaction with Shc. *J. Biol. Chem.* 277:16798–16804.

Vassar, R., B.D. Bennett, S. Babu-Khan, S. Kahn, E.A. Mendiaz, P. Denis, D.B. Teplow, S. Ross, P. Amarante, R. Loeloff, et al. 1999. Beta-secretase cleavage of Alzheimer's amyloid precursor protein by the transmembrane aspartic protease BACE. *Science.* 286:735–741.

Wolfe, M.S., W. Xia, B.L. Ostaszewski, T.S. Diehl, W.T. Kimberly, and D.J. Selkoe. 1999. Two transmembrane aspartates in presenilin-1 required for presenilin endoproteolysis and gamma-secretase activity. *Nature.* 398:513–517.

Yan, R., M.J. Bienkowski, M.E. Shuck, H. Miao, M.C. Tory, A.M. Pauley, J.R. Brashier, N.C. Stratman, W.R. Mathews, A.E. Buhl, et al. 1999. Membrane-anchored aspartyl protease with Alzheimer's disease beta-secretase activity. *Nature.* 402:533–537.

Yang, L.B., K. Lindholm, R. Yan, M. Citron, W. Xia, X.L. Yang, T. Beach, L. Sue, P. Wong, D. Price, et al. 2003. Elevated beta-secretase expression and enzymatic activity detected in sporadic Alzheimer disease. *Nat. Med.* 9:3–4.

Zheng, P., J. Eastman, S. Vande Pol, and S.W. Pimplikar. 1998. PAT1, a microtubule-interacting protein, recognizes the basolateral sorting signal of amyloid precursor protein. *Proc. Natl. Acad. Sci. USA.* 95:14745–14750.